Dendritic Cell Expression of the Signaling Molecule TRAF6 Is Critical for Gut Microbiota-Dependent Immune Tolerance

Daehee Han,[1,7] Matthew C. Walsh,[1] Pedro J. Cejas,[1] Nicholas N. Dang,[1] Youngmi F. Kim,[1] Jihyun Kim,[1] Laetitia Charrier-Hisamuddin,[2] Lillian Chau,[2] Qin Zhang,[3] Kyle Bittinger,[3] Frederic D. Bushman,[3] Laurence A. Turka,[6] Hao Shen,[3] Boris Reizis,[5] Anthony L. DeFranco,[4] Gary D. Wu,[2] and Yongwon Choi[1,7,*]
[1]Department of Pathology and Laboratory Medicine
[2]Division of Gastroenterology
[3]Department of Microbiology
University of Pennsylvania Perelman School of Medicine, Philadelphia, PA 19104, USA
[4]Department of Microbiology and Immunology, University of California, San Francisco, San Francisco, CA 94143, USA
[5]Department of Microbiology and Immunology, Columbia University Medical Center, New York, NY 10032, USA
[6]Department of Medicine, Beth Israel Deaconess Medical Center and Harvard Medical School, Boston, MA 02215, USA
[7]Division of Integrative Biosciences and Biotechnology, Pohang University of Science and Technology, Pohang, Republic of Korea
*Correspondence: ychoi3@mail.med.upenn.edu
http://dx.doi.org/10.1016/j.immuni.2013.05.012

SUMMARY

The intracellular signaling molecule TRAF6 is critical for Toll-like receptor (TLR)-mediated activation of dendritic cells (DCs). We now report that DC-specific deletion of TRAF6 (TRAF6ΔDC) resulted, unexpectedly, in loss of mucosal tolerance, characterized by spontaneous development of T helper 2 (Th2) cells in the lamina propria and eosinophilic enteritis and fibrosis in the small intestine. Loss of tolerance required the presence of gut commensal microbiota but was independent of DC-expressed MyD88. Further, TRAF6ΔDC mice exhibited decreased regulatory T (Treg) cell numbers in the small intestine and diminished induction of iTreg cells in response to model antigen. Evidence suggested that this defect was associated with diminished DC expression of interleukin-2 (IL-2). Finally, we demonstrate that aberrant Th2 cell-associated responses in TRAF6ΔDC mice could be mitigated via restoration of Treg cell activity. Collectively, our findings reveal a role for TRAF6 in directing DC maintenance of intestinal immune tolerance through balanced induction of Treg versus Th2 cell immunity.

INTRODUCTION

Microbial pathogens have long been understood to produce inflammatory stimuli essential to induction of adaptive immune responses, and there is now increasing interest in understanding the relationship between microbiota and maintenance of immune cell tolerance (Maloy and Powrie, 2011; Swiatczak and Rescigno, 2012). Pathogen-associated molecular patterns (PAMPs) derived from pathogenic, as well as commensal, microbiota are recognized by Toll-like receptors (TLRs) that are highly

expressed by dendritic cells (DCs) along the mucosal lining (Maloy and Powrie, 2011; Pulendran et al., 2010). DCs are specialized antigen-presenting cells (APCs) that are capable, under inflammatory conditions, of providing costimulatory signals and efficient antigen presentation through major histocompatibility complex (MHC) to T cells (Steinman, 2012). These functions are critical for an effective adaptive immune response, but DCs are now also recognized as key cellular keepers of immune tolerance (Manicassamy and Pulendran, 2011; Rescigno, 2010). What remains unclear is the degree to which this dual role is balanced by dispatchment of specialized subsets of DCs versus specific tuning of DC-intrinsic signaling mechanisms to affect certain immunologic outcomes. Past attempts to address these issues via ex vivo analyses of DC phenotypes have often been hampered by the keen sensitivity of DCs to external manipulation. The recent development of a transgenic mouse model enabling specific genetic targeting to the DC compartment represents a major step forward in conducting physiologic in vivo analysis of DC function (Caton et al., 2007).

The molecular adaptor protein TRAF6 integrates upstream signals from both MyD88-dependent IL-1R-TLR superfamily pathways, as well as some tumor necrosis factor receptor (TNFR) superfamily members, including CD40 and RANK (Inoue et al., 2007; Walsh et al., 2006). Activation of TRAF6, a nonconventional RING finger E3 ligase, which catalyzes formation of K63-linked ubiquitin chains, results in downstream activation of the NF-κB, MAPK, and PI3K pathways (Deng et al., 2000; Inoue et al., 2007). Activation of TRAF6-dependent signaling is associated with induction of inflammatory gene expression products, including IL-6 and IL-12. We have previously shown that DCs derived from TRAF6-deficient ($Traf6^{-/-}$) mice or $Traf6^{-/-}$ fetal liver cell chimeras exhibit substantial defects in maturation and inflammatory cytokine elaboration in response to IL-1R-TLR superfamily ligands and TNF superfamily members, and that $Traf6^{-/-}$ DCs adoptively transferred into third party hosts possess decreased capability to induce antigen-dependent T cell expansion and interferon-γ (IFN-γ) induction (Kobayashi et al., 2003). However, because $Traf6^{-/-}$ mice die perinatally
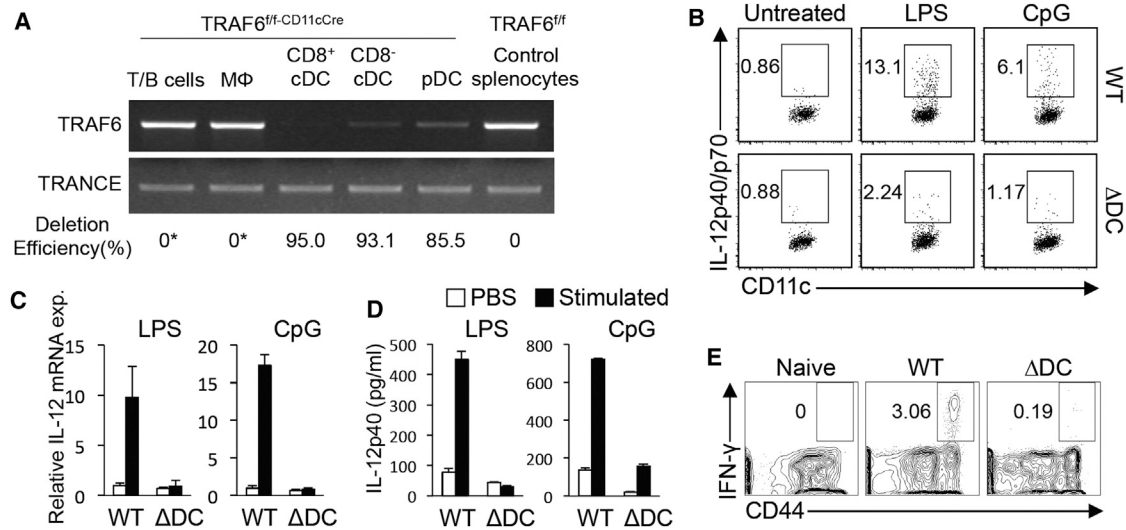
Figure 1. Generation of Mice Lacking TRAF6 Specifically in the DC Compartment

(A) Quantitative PCR of the floxed region of the *Traf6* gene was performed with genomic DNA from TRAF6ΔDC (TRAF6^f/f-CD11cCre) and control (TRAF6^f/f) FACS-sorted cells to measure degree of deletion in various cell types. A sequence from the TRANCE (*Tnfsf11*) gene was used as a control for sample standardization. (*, deletion not detected).

(B) IL-12 expression in wild-type (WT) or TRAF6ΔDC (ΔDC) mice after intravenous injection with PBS, LPS, or CpG. IL-12p40/p70 was detected by intracellular staining for splenocytes isolated at 2 hr after injection. The representative FACS plots were gated on CD11c^hiMHC class II^hi DCs.

(C and D) IL-12p40 mRNA production after in vitro stimulation of MACS-sorted splenic DCs with LPS or CpG. (C) IL-12p40 expression was determined by qPCR from mRNA 1 hr after stimulation. (D) IL-12p40 from culture medium was measured by ELISA 12 hr after stimulation.

(E) Intracellular IFN-γ level was determined from splenocytes 7 days after infection with LCMV. Shown are representative FACS plots gated on CD4^+ T cells. The histograms in (C) and (D) represent mean ± SD. FACS plots in (B) and (E) are representative of at least three separate experiments.

(surviving no longer than about 15 days), and *Traf6^−/−* fetal liver chimeras develop progressive inflammatory disease characterized by massive organ infiltration of Th2-like cells (Chiffoleau et al., 2003), it has not been possible to specifically examine the in situ role of DC-expressed TRAF6 in the context of physiologic immune responses or immune homeostasis.

Therefore, we have generated mice lacking TRAF6 specifically in the DC compartment (TRAF6ΔDC.) We report here that despite defective activation of TRAF6-deficient DCs in peripheral lymphoid organs like the spleen, we have made the striking observation that TRAF6ΔDC mice develop spontaneous loss of immune tolerance in the gut that is associated with both decreased Treg cell numbers and the presence of microbiota. These findings highlight a unique role for TRAF6 in DC function and serve to elucidate the relationship between microbiota and DCs in the maintenance of immune tolerance.

RESULTS

Generation of Mice Lacking TRAF6 Specifically in the DC Compartment

To generate TRAF6ΔDC mice lacking TRAF6 specifically in the DC compartment, we have crossed mice carrying a floxed *Traf6* exon 1 allele (which we have previously described; King et al., 2006) with CD11c-Cre (*Itgax*-Cre) transgenic mice (Caton et al., 2007). DCs sorted from spleens of TRAF6ΔDC mice exhibit specific deletion of TRAF6 compared to other sorted cell types as determined by qPCR of genomic DNA samples (Figure 1A). Specific deletion was further observed in DCs isolated from other tissues as well (data not shown.) To determine whether

splenic DCs from TRAF6ΔDC mice exhibit predicted defective responses to inflammatory stimuli, we measured IL-12 expression in response to both in vivo (Figure 1B) and in vitro (Figures 1C and 1D) treatment with the TLR ligands LPS and CpG DNA and revealed that cytokine production is reduced in the absence of TRAF6. To demonstrate the effect of DC-specific TRAF6 deficiency on T cell activation under inflammatory conditions in vivo, we infected TRAF6ΔDC mice with LCMV and splenic CD4^+ T cells were assayed for CD44 upregulation and IFN-γ production 7 days later, revealing a severely reduced IFN-γ^+ cell population in TRAF6ΔDC mice (Figure 1E). Together, these results demonstrate a requirement of DC-expressed TRAF6 for induction of DC activation in response to pathogenic stimuli.

TRAF6ΔDC Mice Exhibit Spontaneous Small Intestine Enteritis

DCs are important mediators of mucosal immune tolerance (Maloy and Powrie, 2011; Pulendran et al., 2010). Although gut TRAF6ΔDC DC subsets (characterized by CD103 and/or CD11b expression) were found in normal proportions and numbers, and with normal levels of membrane activation markers (see Figures S1C and S1D available online), examination of the gut tissue of TRAF6ΔDC mice revealed that, by 12 weeks of age, TRAF6ΔDC mice begin to exhibit substantially increased tissue length and mass specifically in the small intestine (Figures 2A; Figure S1A). Histological analysis showed signs of spontaneous enteritis, characterized by thickening of the smooth muscle layer, hypertrophy of the intestinal crypts, blunted villi, and increased numbers of both goblet and Paneth cells (Figure S2). There was also evidence of developing fibrosis,
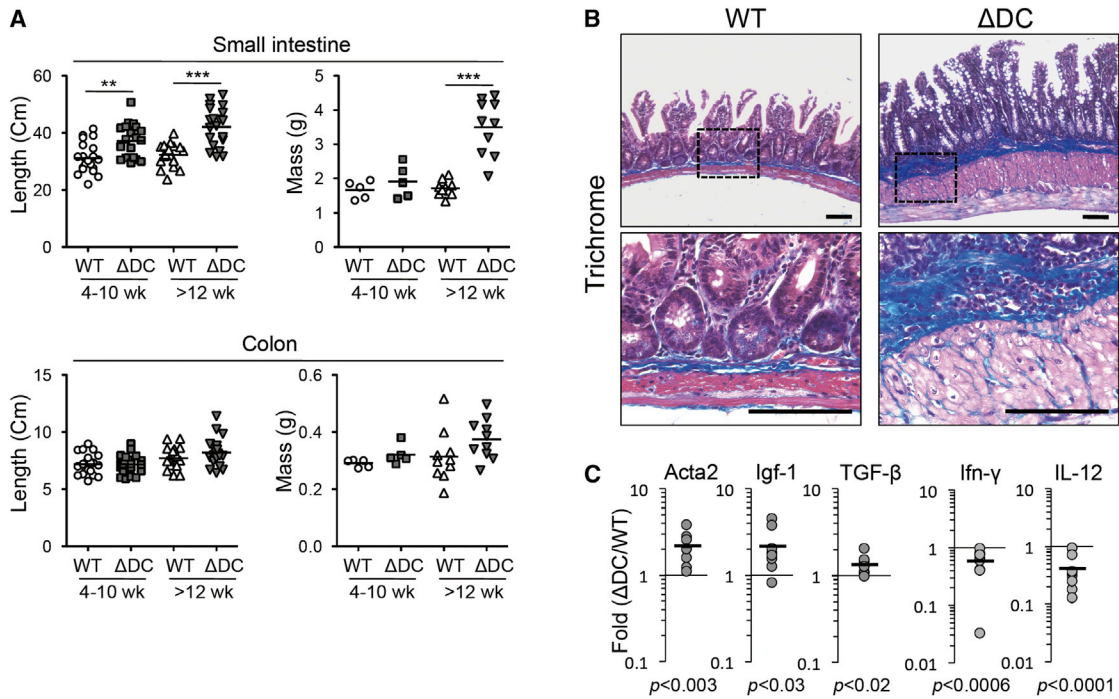
Figure 2. TRAF6ΔDC Mice Exhibit Spontaneous Small Intestine Enteritis

(A) Lengths (n = 20) and masses (n ≥ 5) of small intestines and colons from littermate control (WT) and TRAF6ΔDC (ΔDC) mice organized according to age at sacrifice. Data were analyzed by one-way ANOVA with Tukey's posttest of multiple comparisons.

(B) Trichrome staining was performed on the muscularis propria of the ileum at 27 weeks of age. Collagen (blue, arrows) from Trichrome staining is a marker for gut fibrosis. Smooth muscle layer (arrowheads) corresponds with red staining in sections.

(C) Fold increases in pro- (Acta2, Igf-1, and TGF-β) and anti- (IFN-γ and IL-12) fibrotic markers in mRNA isolated from ileum of TRAF6ΔDC (ΔDC) small intestines were compared to WT (n ≥ 9; ≥ 8-week-old littermate groups). Data were analyzed with two-tailed, paired Student's t tests. **p < 0.01; ***p < 0.001. Scale bars represent 100 μm. n.s., not significant. See also Figures S1–S4.

with muscular hypertrophy and increased collagen staining (Figure 2B). Consistent with this observation, tissue messenger RNA (mRNA) levels of profibrogenic factors Acta2, Igf-1, and transforming growth factor-β (TGF-β) were increased, whereas antifibrogenic (and Th1-related) factors IL-12 and IFN-γ were slightly reduced (Figure 2C). At the same time, similar analyses revealed TRAF6ΔDC colons to be unremarkable (Figure S3). These results reveal a role for DC TRAF6 in maintaining gut homeostasis.

Spontaneous Th2 Cell Responses in the Small Intestine of TRAF6ΔDC Mice

To elucidate potential cellular interactions driving small intestine enteritis in TRAF6ΔDC mice, we crossed TRAF6ΔDC mice to a SCID background. The small intestines of TRAF6ΔDC.SCID mice appear similar to control SCID mice, even past 20 weeks of age, and exhibit substantially reduced levels of fibrotic markers Acta2 and Igf-1 (Figure S4), suggesting that lymphocytes are critical to the development of the TRAF6ΔDC small intestine phenotype. Consistent with these findings, we observed development of lymphadenopathy of TRAF6ΔDC mesenteric lymph nodes with age (Figure S1B). Analysis of serum and fecal immunoglobulin A (IgA) titers, which are associated with B cell activity in the mucosal lining, showed substantial increases in TRAF6ΔDC mice (Figures 3A and 3B). Analysis of small intestine lamina propria (LP) tissue gene expression from TRAF6ΔDC and littermate control mice older than 8 weeks of age revealed sub-

stantial increases in Th2 cell-associated factors IL-13, IL-5, and IL-4 (Figure 3C), whereas colons from the same mice showed no significant increases in expression and the tissue was histologically normal in appearance (data not shown.) To investigate whether these cytokines were being produced by T cells in situ, we performed immunofluorescent staining, which revealed costaining of IL-4 and the T cell marker CD3 in TRAF6ΔDC small intestinal LP (Figure 3D). Further, in TRAF6ΔDC mesenteric lymph nodes we found substantially increased numbers and frequencies of activated and/or memory CD4+ T cells (Figure 3E), as well as more CD4+ T cells capable of producing IL-13—but not IFN-γ—upon in vitro stimulation (Figure 3F). Th2 cell-mediated intestinal phenotypes are sometimes associated with eosinophil infiltration (Blanchard and Rothenberg, 2009). By staining small intestine sections with Sirius Red, we found that TRAF6ΔDC mice exhibit substantially increased eosinophil numbers (Figure 3G), potentially revealing a parallel between the TRAF6ΔDC phenotype and human EGID (eosinophilic gastrointestinal diseases; Lucendo, 2010; Masterson et al., 2011).

Disruption of TRAF6ΔDC Immune Homeostasis Is Gut Microbiota-Dependent

TRAF6 is a key transducer of TLR signaling pathways that are tasked in part with mediating inflammatory and homeostatic interactions between DCs and gut microbiota (Maloy and Powrie,
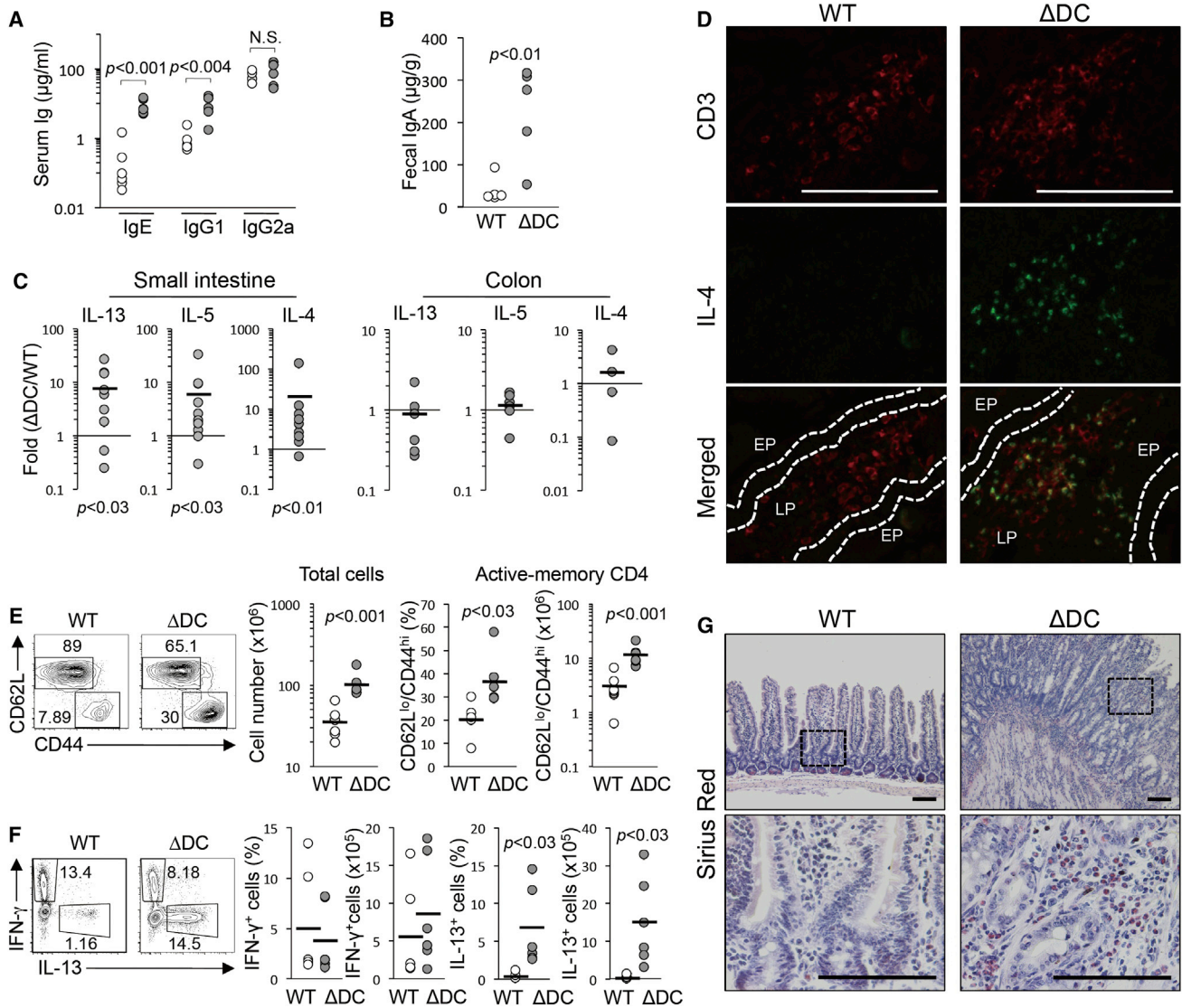
Figure 3. Spontaneous Th2 Cell Responses in the Small Intestine of TRAF6ΔDC Mice

Serum (A) and fecal (B) immunoglobulin isotype levels in mice (n ≥ 5; ≥ 12-week-old littermate groups) were measured by ELISA.

(C) Fold increases (between TRAF6ΔDC mice and paired littermate control mice) in IL-13, IL-5, and IL-4 mRNA expression in small intestine (n ≥ 8) or colon (n ≥ 4) tissue as measured by qPCR.

(D) Double immunofluorescent staining for CD3 and IL-4. EP, epithelial cell lining; LP, lamina propria.

(E and F) Increases in activated/memory CD4$^+$ cells and IL-13$^+$ cells in mesenteric lymph nodes of TRAF6ΔDC mice compared to littermate control mice (WT). FACS plots gated on CD4$^+$ T cells and show population counts and frequencies of (E) naive (CD44^{lo}CD62L^{hi}) versus activated/memory (CD44^{hi}CD62L^{lo}), and (F) IFN-γ$^+$ and IL-13$^+$ cells (n = 6; ≥ 12-week-old littermate groups).

(G) Image of eosinophils (in red) stained with Sirius Red. Eosinophil infiltration is observed in small intestinal sections of TRAF6ΔDC and littermate control (duodenum, 27 weeks old). FACS plots and histogram data are representative of at least three separated experiments. Data in (A) and (B) were analyzed with two-tailed, unpaired Student's t tests. Data in (C), (E), and (F) were analyzed with two-tailed, paired Student's t tests. Scale bars represent 100 μm. See also Figure S1.

2011; Swiatczak and Rescigno, 2012). To determine whether gut microbiota interaction with small intestine DCs is relevant to the observed TRAF6ΔDC phenotype, we treated TRAF6ΔDC and littermate control mice with full-spectrum antibiotics for up to six weeks starting at 14 weeks of age. Intriguingly, we observed that antibiotics-treated TRAF6ΔDC intestines now (as compared to untreated intestines shown in Figure S1A) exhibited grossly normal appearance (Figure S4B) and normal

mean length and mass (Figure 4A). Small intestine mRNA levels of both profibrotic and Th2 cell-associated genes were substantially reduced under antibiotic treatment (as compared to untreated) conditions (Figure 4B). Further, antibiotics-treated mice exhibited substantial reductions in both the frequency and number of IL-13-producing CD4$^+$ T cells isolated from the small intestinal LP (Figure 4C). Finally, histological sections of TRAF6ΔDC small intestine tissue from antibiotics-treated mice
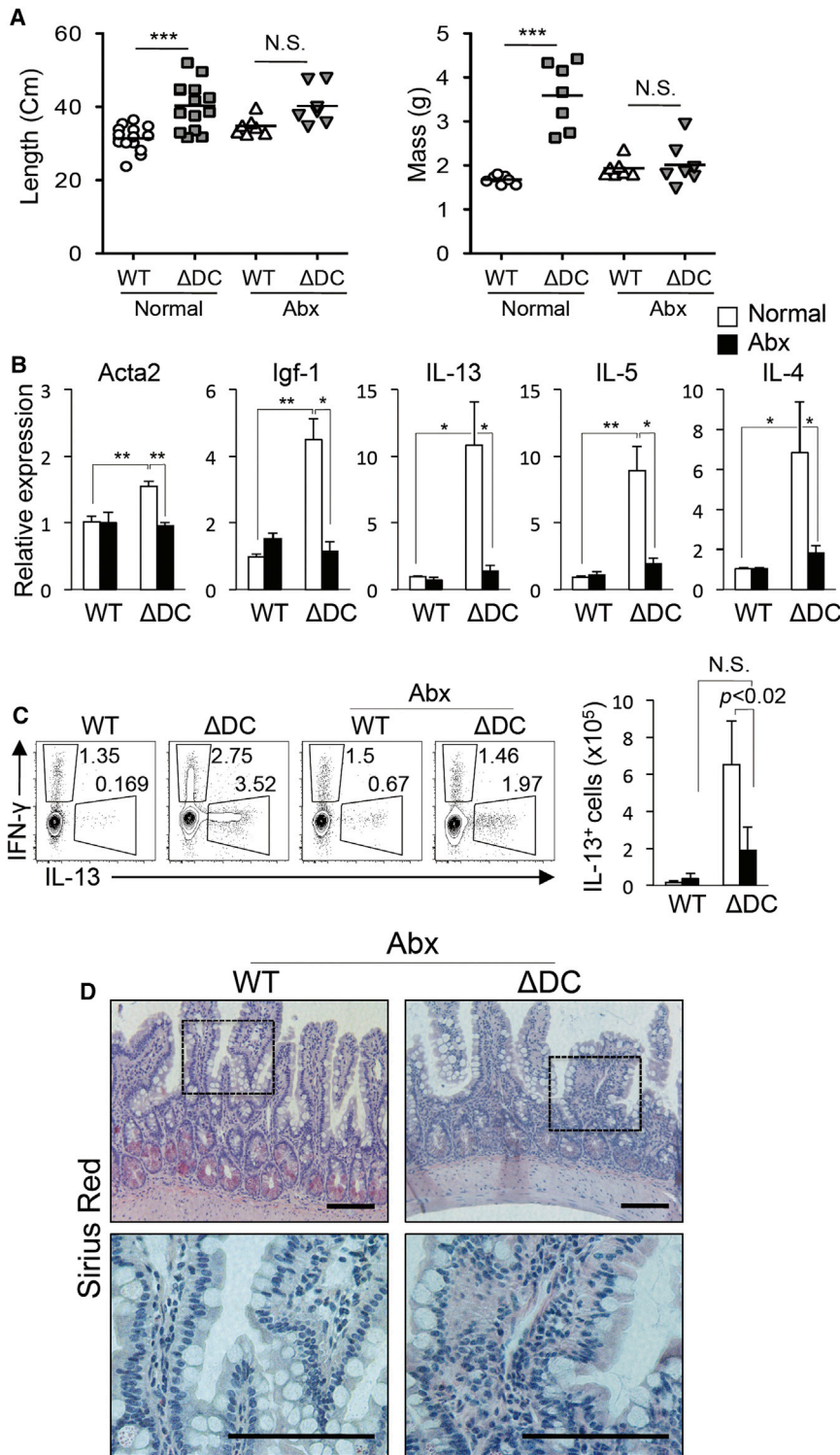
Figure 4. Disruption of TRAF6ΔDC Immune Homeostasis Is Gut Microbiota Dependent

(A) Lengths and masses (n ≥ 7 per group) of small intestines from 8- to 20-week-old littermate-matched control (WT) and TRAF6ΔDC (ΔDC) mice provided untreated or antibiotics-treated (Abx) water for the final 6 weeks. ***p < 0.001.

(B) Fibrosis markers (Acta2 and Igf-1) and Th2 cell cytokines (IL-13, IL-5, and IL-4) mRNA expression levels in the ileum region of small intestines from mice treated with full-spectrum antibiotics (Abx). Histograms (mean ± SD) are representative of three independent experiments.

(C) Intracellular staining for IFN-γ, IL-13, and Foxp3 in mesenteric lymph nodes of antibiotics-treated (Abx) or untreated mice. FACS plots were gated on CD4+ T cells and cell counts of IL-13-producing cells are shown in the histogram. FACS plots are representative of three independent experiments. The histograms represent means ± SD.

(D) Sirius Red staining of the duodenum region of small intestine from antibiotics-treated (Abx) mice. Antibiotic water containing 1 g/L Ampicillin, 1 g/L Neomycin, 0.5 g/L Vancomycin, and 1 g/L Metronidazole was provided ad libitum in water to 14-week-old mice for 6 weeks. Data in (A), (B), and (C) were analyzed by one-way ANOVA with Tukey's posttest of multiple comparisons. *p < 0.05; **p < 0.01. Scale bars represent 100 μm. n.s., not significant. See also Figures S4.

MyD88ΔDC Mice Do Not Phenocopy Aberrant Immune Homeostasis of TRAF6ΔDC Mice

TRAF6 and MyD88 carry out critical nonredundant roles as mediators of TLR signaling (Inoue et al., 2007; Takeda and Akira, 2004), with MyD88-IRAK complexes leading to activation of TRAF6 and subsequently NF-κB and MAPKs. DC-specific MyD88 conditional knockout mice (MyD88ΔDC) utilizing the same CD11c-Cre system that we have employed for TRAF6ΔDC have previously been studied, and although MyD88ΔDC exhibit defects in TLR-mediated activation and induction of Th1-associated immunity (consistent with our observations of TRAF6ΔDC mice), no aberrant immune homeostasis in the gut is reported (Hou et al., 2008). Given the significance of the MyD88-TRAF6 signaling juncture to DC biology (especially in the context of TLR signaling), together with our observations that TRAF6ΔDC phenotypes are substantially influenced by TLR ligand-producing gut microbiota, we decided to reexamine MyD88ΔDC mice side by side with TRAF6ΔDC mice to determine whether previous analyses may have yielded different results based on housing-specific factors (e.g., quantitatively and/or qualitatively distinct intestinal microbiota). Interestingly,

showed Sirius Red staining similar to littermate control mice, suggesting an absence of eosinophil infiltration (Figure 4D). Therefore, aberrant immune homeostasis related to TRAF6-deficient gut DCs is triggered only when commensal microbiota are present.
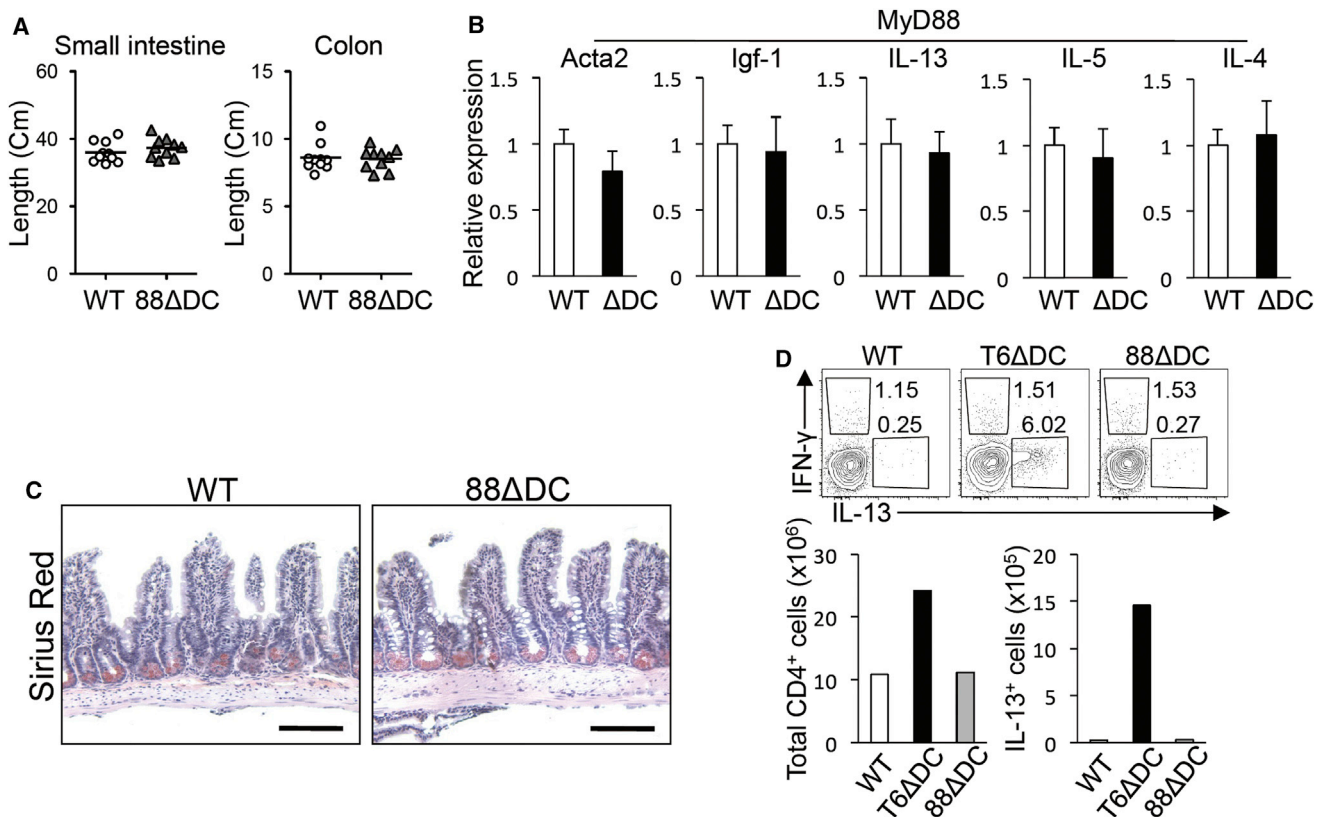
Figure 5. MyD88ΔDC Mice Do Not Phenocopy Aberrant Immune Homeostasis of TRAF6ΔDC Mice

(A) Length of gut was measured in MyD88ΔDC mice (88ΔDC) and littermate controls (WT).

(B) Relative mRNA levels in 20-week-old ileum of MyD88ΔDC mice and littermate controls (WT). The histograms (mean ± SD) are representative of three independent experiments.

(C) Sirius Red staining was performed in the ileum section of small intestine from 20-week-old mice.

(D) FACS plots gated on CD4⁺ T cells showing Intracellular staining for Th1 and Th2 cell cytokines (IFN-γ and IL-13, respectively) in mesenteric lymph nodes from 20-week-old mice and cytokine-producing cell counts. FACS plots and histogram data are representative of three independent experiments. Scale bars represent 100 μm. See also Figure S5.

we found that aged MyD88ΔDC mice exhibited no significant differences in small intestine length versus littermate controls (Figure 5A), no increases in profibrotic or Th2 cell-associated mRNA levels in small intestine tissue samples (Figure 5B), and no apparent eosinophil infiltration of the small intestine (Figure 5C). Further, CD4⁺ T cells isolated from small intestinal LP exhibited frequencies and numbers of IL-13-producing cells no different from littermate controls, and much lower than similar cells isolated at the same time from TRAF6ΔDC mice (Figure 5D), suggesting the existence of a MyD88-independent component to the TRAF6ΔDC small intestine phenotype. We further considered the possibility that genetic manipulation of DC signaling components may exert indirect external population effects on the surrounding commensal microbiota. However, profiling of fecal bacterial communities of control, TRAF6ΔDC, and MyD88ΔDC mice by deep sequencing showed that the most abundant types of bacterial taxa were common among communities of all three genotypes, and their proportions were not significantly different (Figure S5), implying that differences between TRAF6ΔDC and MyD88ΔDC phenotypes are not likely the result of the presence of altered bacteria-derived stimuli in TRAF6ΔDC intestines.

Microbiota-Dependent Reduction in TRAF6ΔDC Small Intestine Treg Cells

One mechanism by which mucosal DCs maintain tolerance is through the induction and maintenance of iTreg cells (Pulendran et al., 2010; Rescigno, 2010), regulatory T cells that acquire their suppressive phenotype in peripheral tissues rather than in the thymus. We analyzed TRAF6ΔDC intestinal LP and found decreased numbers and frequencies of Treg cells (by Foxp3 expression) in mice as young as 6 weeks of age, and importantly, these defects were found in the small intestine, but not the colon (Figure 6A). Consistent with their lack of spontaneous enteritis, MyD88ΔDC mice of similar ages and genders to analyzed TRAF6ΔDC mice were found to have normal Treg cell populations (Figure S6). To determine whether the TRAF6ΔDC Treg cell defect is also dependent on gut microbiota, we again treated mice with full-spectrum antibiotics, but this time started at 4 weeks of age to account for the early presentation of the Treg cell defect. Interestingly, we found that 2 weeks of treatment was sufficient to partially restore the frequency (within the total CD4⁺ T cell population) and completely restore the number of Treg cells located in the TRAF6ΔDC small intestine (Figure 6B). Therefore, defective
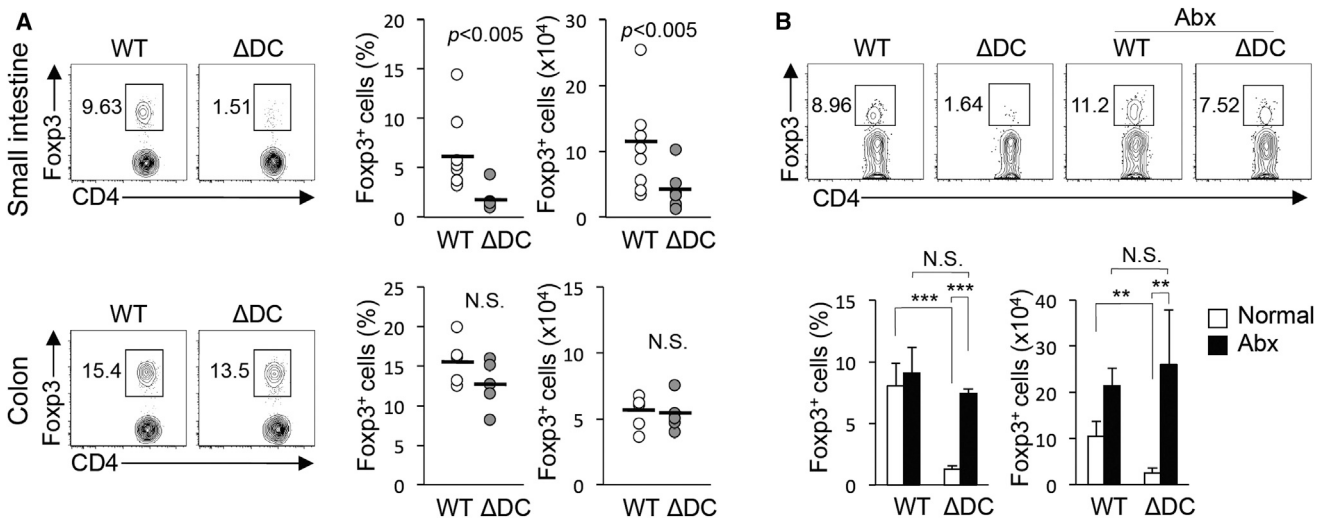
Figure 6. Microbiota-Dependent Reduction in TRAF6ΔDC Small Intestine Treg Cells

(A) FACS plots gated on CD4$^+$ T cells show intracellular staining for small intestine or colon lamina propria lymphocytes from 6- to 8-week-old TRAF6ΔDC and littermate control mice and Foxp3$^+$ as a percentage of CD4$^+$ and cell counts. Data were analyzed with two-tailed, paired Student's t test.

(B) Intracellular staining for Foxp3 in small intestinal lamina propria of antibiotics-treated (Abx) or untreated mice. FACS plots were gated on CD4$^+$ T cells. Water containing 1 g/L Ampicillin, 1 g/L Neomycin, 0.5 g/L Vancomycin, 1 g/L Metronidazole was provided to 4-week-old mice for 2 weeks. The histograms (mean ± SD) were analyzed by one-way ANOVA with Tukey's posttest of multiple comparisons. FACS plots in (A) and (B) are representative of at least three separate experiments. **p < 0.01; ***p < 0.001. N.S., not significant. See also Figures S6 and S7.

TRAF6ΔDC Treg cell induction appears to depend on the presence of microbiota.

Defective DC-Expressed IL-2 and Rescue of Treg Cells via Exogenous IL-2 in TRAF6ΔDC Mice

To uncover potential mechanistic bases for diminished Treg cell numbers in TRAF6ΔDC LP, we investigated the potential roles of cell surface markers and other proteins reportedly involved in the induction of intestinal iTreg cells by DCs. Numerous factors, including Aldh1a2, TGF-β, integrin-α$_v$, and integrin-β$_8$ showed no apparent difference between control and TRAF6ΔDC (Figure S7). This process led us to focus on IL-2, which is not only critical to Treg cell development and maintenance (Malek and Castro, 2010), but which has also been shown to be expressed by DCs (Granucci et al., 2001), and its expression by DCs might play a role in Treg cell maintenance (Kulhankova et al., 2012; Sgouroudis et al., 2011). We have also found that blocking IL-2 or use of IL-2-deficient DCs results in diminished Treg cell conversion (Figure S8). Interestingly, we examined IL-2 expression in control, MyD88ΔDC, and TRAF6ΔDC LP DCs and found that although IL-2 mRNA levels in both control and MyD88ΔDC samples were similar, levels in TRAF6ΔDC LP DCs were dramatically reduced (Figure 7A). TRAF6ΔDC LP DCs similarly exhibited decreased IL-2 protein elaboration during brief ex vivo culture (Figure 7B). Next, we showed that although DCs from TRAF6ΔDC mice are defective inducers of Foxp3 in in vitro Treg cell conversion assays, provision of IL-2 to these cultures had a corrective effect on this defect (Figure 7C). Finally, we similarly showed that defective in vivo model antigen-induced Treg cell conversion of adoptively-transferred TCR transgenic T cells into TRAF6ΔDC recipients could be restored to the higher levels observed in MyD88ΔDC recipients (which are similar to those observed for control recipients) through provision of

bioactive IL-2–αIL-2 complexes (Figure 7D). Together, these findings suggest that the decreased capacity of DCs from TRAF6ΔDC mice to induce the Treg cell phenotype can be overcome by provision of the pro-Treg cell cytokine IL-2 and raises the possibility that DC-expressed IL-2 is required for normal Treg cell homeostasis in the gut.

Defective TRAF6ΔDC iTreg Cell Induction Is Linked to Aberrant Th2 Cell Development

Decreased Treg cell numbers in the small intestine raised the possibility that Treg cell maintenance and/or iTreg cell induction are defective in TRAF6ΔDC mice. To address the first possibility, we sorted GFP-expressing peripheral Treg cells from transgenic mice expressing GFP under the control of the Foxp3 promoter (Fontenot et al., 2005) and transferred these cells into control or TRAF6ΔDC recipient mice. After 1 week, the populations of transferred cells were identified by GFP expression and enumerated. Whereas endogenous levels of TRAF6ΔDC Treg populations were decreased (as expected: Figure 7E, left), the transferred populations appeared at normal levels (Figure 7E, middle and right.) Therefore, to address the alternative possibility of defective iTreg cell induction, we adoptively transferred sorted naive (CD44^{lo}CD62L^{hi}CD25$^-$) Thy1.1 congenic OVA-specific OT-II CD4$^+$ T cells into TRAF6ΔDC or littermate control mice followed by 5 days of oral administration of OVA peptide. By using congenic markers, transferred cells were identified after 1 week and Foxp3 staining revealed that TRAF6ΔDC recipient mice exhibit substantially reduced capability to induce Treg cells in response to model oral antigen (Figure 7F).

These findings raised the possibility that reduced Treg cell function in TRAF6ΔDC mice may be linked to spontaneous induction of intestinal Th2 cell immunity. To restore robust Treg cell function experimentally, we crossed Foxp3-GFP mice with
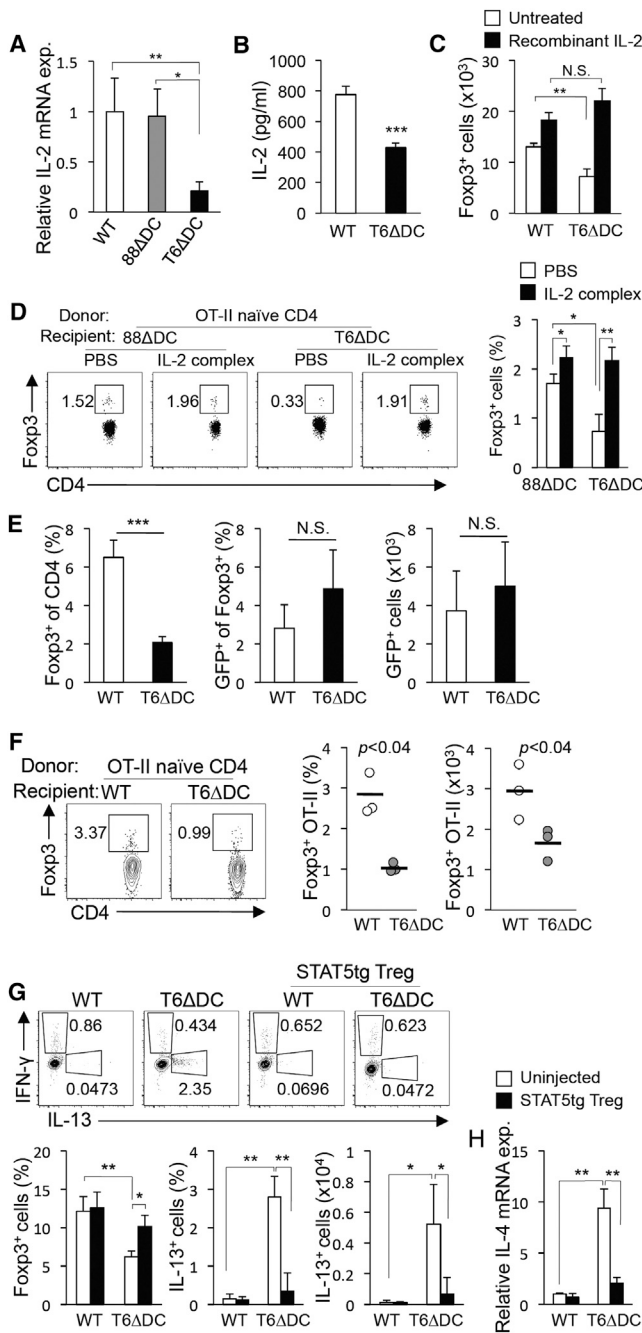
transgenic mice expressing a constitutively active form of the pro-Treg cell transcription factor STAT5b (Burchill et al., 2003) (Foxp3-GFP.STAT5bCA) and then adoptively transferred sorted Foxp3-GFP$^+$ Treg cells from those mice into either TRAF6ΔDC or littermate control recipients. Foxp3-GFP.STAT5bCA Treg cells were used because they were obtainable in large numbers, and, we reasoned, would be more stable as a population (capable of reliably providing Treg cell activity) once transferred. This was important because the TRAF6ΔDC gut phenotype developed over an extended time period. Four weeks after transfer, we observed that TRAF6ΔDC mice that had received STAT5bCA Treg cells had partially restored Treg cell numbers, and, more importantly, exhibited reduced frequencies and numbers of small intestinal LP Th2 cell cells and cytokine expression (Figures 7G and 7H). These findings suggested a direct link between Treg cell function and spontaneous development of aberrant gut immune responses in TRAF6ΔDC mice.

DISCUSSION

DCs are important for both activation of inflammatory T cell immune responses and maintenance of T cell tolerance. By generating mice that specifically lack DC-expressed TRAF6, we have been able to characterize a new role for TRAF6 in directing DC maintenance of intestinal immune tolerance. Although TRAF6ΔDC mice were found to exhibit some predicted (given our previous work with Traf6$^{-/-}$ DCs) phenotypes, such as defective induction of TLR-mediated peripheral Th1 cell-associated responses, we were surprised to find that these mice also exhibit defective intestinal iTreg cell induction and subsequent spontaneous Th2 cell-associated disruption of immune homeostasis. Intriguingly, these TRAF6ΔDC phenotypes were found to be dependent on the presence of gut microbiota, whereas mice lacking MyD88, the signaling protein that links TLRs to TRAF6, in DCs (MyD88ΔDC) did not exhibit any signs of disease onset or decreased Treg cell numbers. Furthermore, we have shown that LP DCs harvested from TRAF6ΔDC mice exhibit dramatically reduced levels of IL-2 mRNA and that IL-2 provision

Figure 7. Treg Homeostasis and Gut Immune Tolerance in TRAF6ΔDC Mice Is Linked to Regulation of DC-Expressed IL-2

(A) IL-2 mRNA expression levels in MACS-purified lamina propria DCs from WT, MyD88ΔDC (88ΔDC), and TRAF6ΔDC (T6ΔDC) mice.

(B) ELISA of IL-2 proteins levels elaborated by WT and TRAF6ΔDC (ΔDC) lamina propria DCs cultured for 12 hr with 50 ng/mL PMA and 500 ng/mL ionomycin. ***p < 0.001.

(C) Counts of Foxp3$^+$ cells converted from naive-effector OT-II CD4$^+$ T cells after 4 days culture with purified lamina propria DCs (5 × 10^4 T cells and 5 × 10^3 DCs) from WT or TRAF6ΔDC (T6ΔDC) (1 μM OVA 323–332 and 1 ng/ml TGF-β in all cultures) in the presence (IL-2$^+$) or absence (IL-2$^-$) of 10 U/mL recombinant IL-2.

(D) FACS plots and histograms show the frequencies of Foxp3$^+$ OT-II donor cells in mesenteric lymph nodes after 5 days of OVA feeding. MyD88ΔDC

(88ΔDC) and TRAF6ΔDC (T6ΔDC) mice were used as recipients. IL-2-mAb complex (IL-2 complex) was injected as indicated for the first 3 days of OVA-feeding.

(E) FACS sorted Foxp3-GFP$^+$ cells (0.5 × 10^6) were transferred to WT or TRAF6ΔDC recipients. Cells were isolated and analyzed from small intestinal lamina propria 7 days after transfer. The histograms show the Foxp3-GFP$^+$ (donor) cells as a ratio of total Foxp3$^+$ cells and counts of Foxp3-GFP$^+$ cells in the gut (n = 3).

(F) Intracellular staining and cell counts of converted donor OT-II cells recovered from mesenteric lymph nodes of mice fed OVA protein for 5 days. FACS plots depict gated CD45.1$^+$ (donor marker) and CD4$^+$ T cells.

(G and H) STAT5bCA transgenic Foxp3-GFP$^+$ regulatory T cells (STAT5tg Treg cell) were transferred to TRAF6ΔDC and littermate control recipients. (G) FACS plots showing Intracellular staining for Th1 and Th2 cell cytokines (IFN-γ and IL-13, respectively) 4 weeks after transfer. The percentages and counts for Foxp3$^+$ or IL-13$^+$ from CD4$^+$ T cells in mesenteric lymph nodes, and (H) Th2 cell cytokine (IL-4) mRNA expression level from ileum of both adoptively transferred and no transfer control groups. FACS plots and graphs are representative of at least three separate experiments. The histograms are represented as mean ± SD. Data in (C), (D), and (G) were analyzed by one-way ANOVA with Tukey's posttest of multiple comparisons. *p < 0.05; **p < 0.01; ***p < 0.001. n.s., not significant. See also Figure S8.

can rescue defective iTreg cell induction by TRAF6ΔDC DCs in multiple contexts. These findings represent a potentially significant link between TRAF6 signaling pathways and the production of cytokines functionally relevant to the maintenance of immune tolerance. Further, in light of recent work by Kulhankova et al. regarding juxtacrine relationships of IL-2 with DCs and Treg cells (Kulhankova et al., 2012), it will be especially interesting to further investigate the potential role of TRAF6-dependent signaling in this relationship. It is also important to point out that identification of a potential role for DC-expressed IL-2 in TRAF6ΔDC Treg cell homeostasis does not exclude the possibility that other Treg cell-associated cytokines, such as IL-10, are also relevant. However, at this time, we have not identified any irregular expression patterns of such factors in DCs isolated from TRAF6ΔDC mice.

Decoding the complex signaling networks that govern the relationships between DC-mediated tolerance and immunity, and being able to do so in a physiologic setting (and avoiding the difficulties associated with studying DCs ex vivo), represented significant motivations for generating and studying TRAF6ΔDC mice. It is instructive to consider our observations of the in vivo relevance of DC-expressed TRAF6 in the context of some TRAF6-associated signaling factors that have been similarly analyzed. To begin with, because of the divergent phenotypes described above in TRAF6ΔDC and MyD88ΔDC mice in the presence of TLR ligand-bearing microbiota, we infer: (1) that TLRs activate a MyD88-independent, TRAF6-dependent pathway that serves to promote a tolerogenic phenotype in DCs (this pathway could involve the TLR adaptor TRIF [Takeda and Akira, 2004] and/or the NOD2-RIP2 signaling complex [Brand, 2009; Fritz et al., 2011]); (2) that microbiota act directly or indirectly on DCs through pattern-recognition receptor (PRR)-independent pathways (such as extracellular ATP, which has been shown to act through P2X and P2Y receptors to modulate regulation of immune tolerance by DCs [Atarashi et al., 2008; Idzko et al., 2007]); or (3) that TLRs stimulate production of factors by non-DCs (e.g., epithelial, Paneth, goblet, other lymphoid or myeloid cells) that then act on DCs through known TRAF6-dependent, MyD88-independent pathways (e.g., TGF-β, CD40L, RANKL, IL-25 [Chang and Dong, 2011; Landström, 2010; Walsh et al., 2006]).

TAK1 is the primary kinase activated by TRAF6, but TAK1ΔDC mice that lack TAK1 in the DC compartment are not reported to develop a similar gut phenotype (Wang et al., 2007). However, TAK1ΔDC mice do exhibit a Treg cell defect. The reason TRAF6ΔDC mice exhibit loss of gut immune tolerance in addition to the similar Treg cell phenotype is likely because DCs in TRAF6ΔDC mice retain sufficient TAK1 activity to avoid the massive survival defect of TAK1ΔDC DCs that would preclude the development of Th2 cells. Unlike TAK1, the ubiquitin-editing molecule A20 is a negative regulator of TRAF6-mediated signaling (Shembade et al., 2010). Recent reports describe mice lacking DC-expressed A20 (A20ΔDC) as developing spontaneous Th1-associated peripheral autoimmunity (Hammer et al., 2011; Kool et al., 2011), and one study identifies the DC-intrinsic pathway responsible for T cell expansion and inflammatory cytokine elaboration as being MyD88-dependent (and therefore, possibly TRAF6-dependent). Consistent with an inverted phenotype (in relation to TRAF6ΔDC), Treg cell numbers

in A20ΔDC mice are reported to be normal (Hammer et al., 2011) or even increased (Kool et al., 2011).

TRAF6 is also involved in TGFβR signaling (Landström, 2010), primarily through activation of TAK1 (Sorrentino et al., 2008). Recent reports indicate that complete ablation of TGFβR1-ALK-5 signaling in DCs results in loss of Langerhans cells (Kel et al., 2010), while DC-specific deletion of αvβ8 integrin, which activates the precursor form of TGF-β, reveals a phenotype bearing some similarity to TRAF6ΔDC, including age-related development of inflammatory bowel disease associated with decreased gut Treg cells (though in the colon rather than the small intestine) (Travis et al., 2007). These findings may imply a role for the TRAF6-specific component of TGFβR signaling in DCs for maintaining mucosal homeostasis.

One of the most curious features of the TRAF6ΔDC gut phenotype is the exacerbating role that gut microbiota play. The fact that depletion of commensal bacteria increased small intestinal LP Treg cells seems to contrast recent findings that commensal bacteria boost gut Treg cell numbers (Atarashi et al., 2011), though these differences may be explained by the fact that these studies were performed for Treg cells in the colon, where commensal-related stimuli are substantially higher than and qualitatively different from the small intestine (Santaolalla et al., 2011; Swiatczak and Rescigno, 2012). Additionally, it is possible that TRAF6 expression in DCs differentially impacts the distribution between the small and large intestines of DC subsets. Specifically, the major subset of mucosal DCs responsible for inducing iTreg cells, the vitamin A-metabolizing CD103^{+} subset, is present at higher numbers in the small intestine (Agace and Persson, 2012) and might be more dependent on TRAF6-dependent signals. The primary defect in TRAF6ΔDC mice might derive first from failure to sufficiently induce small intestine iTreg cells, though thus far we have found TRAF6ΔDC CD103^{+} DCs present in normal numbers expressing normal levels of Retinaldehyde dehydrogenases RALDH1 and RALDH2 (data not shown).

It should also be noted that although we have not identified any phenotypic differences in small intestinal DCs in TRAF6ΔDC mice that might explain why these mice exhibit an iTreg cell defect and Th2 cell-associated autoimmunity, there are certain caveats attached to DC analysis in the gut. First, regarding enumeration, preps are relatively complex and can lead to significant variability between labs and even within labs (Rescigno, 2011). This difficulty must be given special consideration in the case of TRAF6ΔDC because the small intestine tissues become enlarged and fibrotic with disease onset, thereby altering, with respect to control mice, expectations about DC prep efficiency. Second, beyond CD103 and CD11b, there are numerous other markers, including many chemokine receptors (e.g., CX3CR1 and CCR7, as well as CD70), which identify specialized DC subsets. It is difficult to determine, therefore, whether relevant defects in TRAF6ΔDC DCs exist in specific subsets that constitute a minority population. Alternatively, it is possible that disease in TRAF6ΔDC mice is mediated by a DC subset not yet characterized. Clearly, additional effort will be required to determine the specific nature of the relevant cellular and signaling defect(s) in TRAF6ΔDC mice.

Overall, the TRAF6ΔDC mouse dramatically identifies a novel example of a DC signaling mediator that is critical for activation of the immune response in one anatomic and stimulatory context

and critical for maintaining immune homeostasis in another. We believe that this unusual status makes TRAF6ΔDC a valuable model for further elucidating, in a physiologic setting, the mechanisms employed by DCs to balance active immunity and tolerance.

EXPERIMENTAL PROCEDURES

Mice

TRAF6ΔDC and MyD88ΔDC mice were generated by crossing mice carrying floxed alleles of *Traf6* (King et al., 2006) or *MyD88* (Hou et al., 2008) with CD11c Cre transgenic mice (Caton et al., 2007). All mice were backcrossed to B6 background more than ten generations. OT-II transgenic (B6.Cg-Tg [TcraTcrb]425Cbn/J), SCID (B6.CB17-Prkdc^{scid}/SzJ), and congenic (CD45.1, B6.SJL-*Ptprc^a Pepc^b*/BoyJ) mice were purchased from Jackson laboratories. STAT5b-CA transgenic mice (Burchill et al., 2003), Foxp3-GFP mice (Fontenot et al., 2005), and IL-2-GFP knock-in mice (McKarns and Schwartz, 2008; Naramura et al., 1998) were kind gifts from M.A. Farrar (University of Minnesota), A.Y. Rudensky (Sloan Kettering), and Ronald Schwartz (NIH), respectively. All experimental pairs of mice were cohoused. Mouse care and experimental procedures were performed in accordance with protocols from Institutional Animal Care and Use Committees of the University of Pennsylvania.

Buffers and Media

Sort buffer containing 2% FBS and 0.7 mM EDTA was used to prepare, stain, and wash isolated cells. Complete RPMI-1640 medium containing 10% FBS, 10 U/ml Penicillin, 10 μg/ml Streptomycin, 2 mM L-glutamin (Invitrogen), and 50 μM β-mercapotethanol (Sigma) was used for cell culture. Gey's solution composed of 155 mM NH_4Cl (Sigma) and 10 mM $KHCO_3$ (Sigma) was used for red blood cell lysis.

Quantitative PCR

Tissues or purified cells were homogenized in TRIzol (Invitrogen) after freezing in liquid nitrogen. cDNAs were established by using Superscript III (invitrogen) and random hexamer (QIAGEN). TaqMan gene probes were used with TaqMan Universal PCR Master Mix (Applied Biosystems) and run on 7300 Realtime PCR System (Applied Biosystems): 2 min at 50°C, 10 min at 95°C, 50 cycles of 15 s 95°C, 1 min at 60°C, and signals were detected during annealing step (60°C). Relative mRNA expression levels of all samples were normalized to 18S mRNA. The TaqMan gene probes (Applied Biosystems) used: *Acta2* (Mm01546113_m1), *Igf1* (Mm00439560_m1), *Tgfb1* (Mm00441724_m1), *Ifng* (Mm01168134_m1), *Il2* (Mm00434256_m1), *Il12b* (Mm99999067_m1), *Il13* (Mm99999190_m1), *Il5* (Mm00439646_m1), *Il4* (Mm00445259_m1), and 18S ribosomal RNA (Hs99999901_s1).

ELISA

For serum immunoglobulin levels, serum was diluted to 1:10,000–100,000 and immunoglobulin isotype levels measured by eBioscience ELISA kit. For fecal IgA, feces were weighed and homogenized in 10-fold (v/w) PBS containing 0.01% NaN_3. Supernatants were diluted 1:1000 after centrifuging at 4°C and 10,000 rpm for 5 min. IgA level was determined by eBioscience ELISA kit. For IL-2 detection, 3×10^4 DCs (purified from small intestine LP with anti-CD11c MACS beads, Miltenyi Biotech) per triplicate well were stimulated with 500 ng/ml ionomycin and 50 ng/ml PMA (Sigma) for 12 hr. Supernatant concentration of IL-2 was determined with an ELISA kit according to manufacturer instructions (eBioscience). Purified α-IL-2 (JES6-aA12) was used for capture and biotin-conjugated α-IL-2 (JES6-5H4) for detection.

Cell Isolation

Single cells were isolated from spleen and mesenteric lymph nodes by mechanical disruption on 70 μm cell strainers (BD). For small intestinal LP lymphocyte (LPL) isolation, epithelial cells were removed by incubation in stripping RPMI-1640 medium containing 10% FBS, 5 mM EDTA, 1 mM DTT, and 20 mM HEPES at 37°C for 15 min in shaker. The remaining pieces were minced and incubated in serum-free RPMI-1640 medium containing 52 U/ml Liverase TM (Roche), 50 μg/ml DNaseI (Sigma), and 20 mM HEPES at 37°C for 15 min while shaking. For T cell enrichment, LPLs were separated with Percoll

gradient (GE Healthcare). Cells were collected at the interface between 40% and 70% after centrifuging at 2,500 rpm at room temperature for 20 min with no brake. For DC enrichment, 145 μg/ml Histodenz (Sigma) dissolved in sort buffer was used at 2,500 rpm, 4°C for 15 min with no brake. For gene expression assay, LP dendritic cells (LpDCs) were isolated by MACS purification (Miltenyi Biotec) by using magnetic bead-conjugated anti-CD11c antibody.

Flow Cytometry

We used 1×10^6 cells for surface staining in FACS buffer containing α-CD16/32 (2.4G2) and LIVE/DEAD dye (Invitrogen) with combinations of fluorochrome-conjugated antibodies including CD44 (IM7), CD62L (MEL-14), CD25 (PC61.5), CD8 (53-6.7), CD4 (RM4-5), I-A^b (AF6-120.1), CD45.1 (A20), CD45.2 (104), CD11b (M1/70), CD11c (HL3), B220 (RA3-6B2), CD90.2 (53-2.1), and CD103 (2E7). For intracellular staining, cells were stimulated in round-bottom 96-well plates with complete RPMI1640 medium containing 500 ng/ml Ionomycin and 5 ng/ml PMA (Sigma) in the presence of Brefeldin A (BD) for the last 3 hr. After surface staining, the cells were fixed and permeabilized with fixation/permeabilization reagent (eBioscience) and stained with intracellular protein-specific antibodies reconizing IL-12p40/p70 (C15.6), IL-13 (eBio13A), IFN-γ (XMG1.2), and Foxp3 (FJK-16 s). All stained samples were analyzed on an LSRII flow cytometer (BD) and the raw data were calculated and visualized with FlowJo software (Tree Star). All of the antibodies were purchased from BD or eBioscience.

LCMV infection

We administered 2×10^5 PFU of LCMV-Armstrong to mice by intraperitoneal injection. We stimulated 1×10^6 isolated cells from spleen of the mice 7 days after infection by PMA and ionomycin with Brefeldin A treatment for the last 3 hr. After surface marker staining with CD4 and CD44 antibodies, the cells were fixed and permeabilzed by BD Cytofix/Cytoperm Fixation and Permeabilization Solution kit for intracellular staining with IFN-γ antibody.

Histology and Immunofluorescence

Intestinal specimens were cut longitudinally and formed into inside-out Swiss rolls. Paraffin-embedded sections were performed after fixation in 10% Formalin solution (Fisher Diagnostics). Trichrome staining and Sirius Red staining were performed by the Penn Center for Molecular Studies in Digestive and Liver Diseases. Briefly, for Sirius Red staining, hematocylin was used for nucleus staining, and Sirius Red solution was used for eosinophil staining. Trichrome staining was used for staining muscle, cytoplasm, and collagen. For immunofluorescence staining, antigen retrieval of paraffin slides was performed in boiled 0.01 M sodium citrate buffer (pH 6.0) followed by deparaffinization and rehydration. Primary staining with α-CD3 (ab5690, Abcam) and α-IL-4 (BVD4-1D11, Abcam) was performed overnight at 4°C after specimens were blocked with 5% host serum of secondary antibodies. Specimens were examined by using a fluorescence microscope (Olympus) after staining with fluorochrome-conjugated secondary antibodies including Alexa Fluor 488 α-rat IgG (A21208, Invitrogen) and Alexa Fluor 568 α-rabbit IgG (A10042, Invitrogen) and then mounting.

Antibiotic Treatment

Full-spectrum antibiotic treatment was supplied for 2–6 weeks in drinking water containing ampicillin (1 g/L, Cellgro), vancomycin (0.5 g/L, Calbiochem), neomycin sulfate (1 g/L, Calbiochem), and metronidazole (1 g/L, Santa Cruz Biotechnology). The antibiotic solution was refreshed every 4 days.

In Vitro Treg Cell Conversion

We mixed 5×10^4 naive CD4 OT-II cells isolated by FACS Aria cell sorter (BD) and 5×10^3 LpDCs a 96 well round-bottom plate with 1 μM OVA 323–332 and 1 ng/ml TGF-β. After 4 days, cells were counted, fixed and permeabilized with fixation/permeabilization reagent (eBioscience), and stained for surface markers and Foxp3. Stained cells were analyzed on an LSRII flow cytometer (BD).

IL-2-mAb Complex Treatment

Naive congenic OT-II (CD45.1$^+$CD4$^+$CD62L^{hi}CD44^{lo}CD25$^-$) cells isolated with a FACS Aria cell sorter (BD) were transferred intravenously into TRAF6ΔDC or

gender and age-matched control recipients (1 × 10^6 donor cells per mouse). We orally provided 5 mg OVA protein (Sigma) dissolved in PBS to recipients for 5 consecutive days starting 24 hr after transfer. IL-2-mAb complex was prepared in PBS mixed with 1 μg IL-2 (R&D) and 5 μg anti-IL-2 mAb (clone JES6-1; gift from Charles D. Surh [Webster et al., 2009]). The complex was injected intraperitoneally on a daily basis during the first 4 days of OVA treatment. The donor cells were harvested and analyzed from mesenteric lymph nodes on day 6.

In Vivo Treg cell Conversion

Congenic OT-II naive (CD45.1$^+$CD4$^+$CD62L^{hi}CD44^{lo}CD25$^−$) cells isolated with a FACS Aria cell sorter (BD) were transferred intravenously into TRAF6ΔDC or gender-matched littermate control recipients (1 × 10^6 donor cells per mouse). We orally provided 5 mg OVA protein (Sigma) dissolved in PBS to recipients for 5 days in a row from the following day of transfer. Cells were harvested from mesenteric lymph nodes and analyzed on day 6.

Adoptive Transfer of Treg Cells

Single cells were isolated from spleen and lymph nodes of Foxp3-GFP mice or STAT5b transgenic Foxp3-GFP mice. CD4, GFP double-positive cells were collected with a FACS Aria cell sorter (BD), and 0.5–× 10^6 cells injected intravenously to each recipient. Mice were sacrificed and analyzed after 4 weeks.

Statistics

Prism software (GraphPad) and either an unpaired or paired Student's t test were used for data analysis. p values less than 0.05 were considered significant.

REFERENCES

Agace, W.W., and Persson, E.K. (2012). How vitamin A metabolizing dendritic cells are generated in the gut mucosa. Trends Immunol. 33, 42–48.

Atarashi, K., Nishimura, J., Shima, T., Umesaki, Y., Yamamoto, M., Onoue, M., Yagita, H., Ishii, N., Evans, R., Honda, K., and Takeda, K. (2008). ATP drives lamina propria T(H)17 cell differentiation. Nature 455, 808–812.

Atarashi, K., Tanoue, T., Shima, T., Imaoka, A., Kuwahara, T., Momose, Y., Cheng, G., Yamasaki, S., Saito, T., Ohba, Y., et al. (2011). Induction of colonic regulatory T cells by indigenous Clostridium species. Science 331, 337–341.

Blanchard, C., and Rothenberg, M.E. (2009). Biology of the eosinophil. Adv. Immunol. 101, 81–121.

Brand, S. (2009). Crohn's disease: Th1, Th17 or both? The change of a paradigm: new immunological and genetic insights implicate Th17 cells in the pathogenesis of Crohn's disease. Gut 58, 1152–1167.

Burchill, M.A., Goetz, C.A., Prlic, M., O'Neil, J.J., Harmon, I.R., Bensinger, S.J., Turka, L.A., Brennan, P., Jameson, S.C., and Farrar, M.A. (2003). Distinct effects of STAT5 activation on CD4+ and CD8+ T cell homeostasis: development of CD4+CD25+ regulatory T cells versus CD8+ memory T cells. J. Immunol. 171, 5853–5864.

Caton, M.L., Smith-Raska, M.R., and Reizis, B. (2007). Notch-RBP-J signaling controls the homeostasis of CD8- dendritic cells in the spleen. J. Exp. Med. 204, 1653–1664.

Chang, S.H., and Dong, C. (2011). Signaling of interleukin-17 family cytokines in immunity and inflammation. Cell. Signal. 23, 1069–1075.

Chiffoleau, E., Kobayashi, T., Walsh, M.C., King, C.G., Walsh, P.T., Hancock, W.W., Choi, Y., and Turka, L.A. (2003). TNF receptor-associated factor 6 deficiency during hemopoiesis induces Th2-polarized inflammatory disease. J. Immunol. 171, 5751–5759.

Deng, L., Wang, C., Spencer, E., Yang, L., Braun, A., You, J., Slaughter, C., Pickart, C., and Chen, Z.J. (2000). Activation of the IkappaB kinase complex by TRAF6 requires a dimeric ubiquitin-conjugating enzyme complex and a unique polyubiquitin chain. Cell 103, 351–361.

Fontenot, J.D., Rasmussen, J.P., Gavin, M.A., and Rudensky, A.Y. (2005). A function for interleukin 2 in Foxp3-expressing regulatory T cells. Nat. Immunol. 6, 1142–1151.

Fritz, T., Niederreiter, L., Adolph, T., Blumberg, R.S., and Kaser, A. (2011). Crohn's disease: NOD2, autophagy and ER stress converge. Gut 60, 1580–1588.

Granucci, F., Vizzardelli, C., Pavelka, N., Feau, S., Persico, M., Virzi, E., Rescigno, M., Moro, G., and Ricciardi-Castagnoli, P. (2001). Inducible IL-2 production by dendritic cells revealed by global gene expression analysis. Nat. Immunol. 2, 882–888.

Hammer, G.E., Turer, E.E., Taylor, K.E., Fang, C.J., Advincula, R., Oshima, S., Barrera, J., Huang, E.J., Hou, B., Malynn, B.A., et al. (2011). Expression of A20 by dendritic cells preserves immune homeostasis and prevents colitis and spondyloarthritis. Nat. Immunol. 12, 1184–1193.

Hou, B., Reizis, B., and DeFranco, A.L. (2008). Toll-like receptors activate innate and adaptive immunity by using dendritic cell-intrinsic and -extrinsic mechanisms. Immunity 29, 272–282.

Idzko, M., Hammad, H., van Nimwegen, M., Kool, M., Willart, M.A., Muskens, F., Hoogsteden, H.C., Luttmann, W., Ferrari, D., Di Virgilio, F., et al. (2007). Extracellular ATP triggers and maintains asthmatic airway inflammation by activating dendritic cells. Nat. Med. 13, 913–919.

Inoue, J., Gohda, J., and Akiyama, T. (2007). Characteristics and biological functions of TRAF6. Adv. Exp. Med. Biol. 597, 72–79.

Kel, J.M., Girard-Madoux, M.J., Reizis, B., and Clausen, B.E. (2010). TGF-beta is required to maintain the pool of immature Langerhans cells in the epidermis. J. Immunol. 185, 3248–3255.

King, C.G., Kobayashi, T., Cejas, P.J., Kim, T., Yoon, K., Kim, G.K., Chiffoleau, E., Hickman, S.P., Walsh, P.T., Turka, L.A., and Choi, Y. (2006). TRAF6 is a T cell-intrinsic negative regulator required for the maintenance of immune homeostasis. Nat. Med. 12, 1088–1092.

Kobayashi, T., Walsh, P.T., Walsh, M.C., Speirs, K.M., Chiffoleau, E., King, C.G., Hancock, W.W., Caamano, J.H., Hunter, C.A., Scott, P., et al. (2003). TRAF6 is a critical factor for dendritic cell maturation and development. Immunity 19, 353–363.

Kool, M., van Loo, G., Waelput, W., De Prijck, S., Muskens, F., Sze, M., van Praet, J., Branco-Madeira, F., Janssens, S., Reizis, B., et al. (2011). The ubiquitin-editing protein A20 prevents dendritic cell activation, recognition of apoptotic cells, and systemic autoimmunity. Immunity 35, 82–96.

Kulhankova, K., Rouse, T., Nasr, M.E., and Field, E.H. (2012). Dendritic cells control CD4+CD25+ Treg cell suppressor function in vitro through juxtacrine delivery of IL-2. PLoS ONE 7, e43609.

Landström, M. (2010). The TAK1-TRAF6 signalling pathway. Int. J. Biochem. Cell Biol. 42, 585–589.

Lucendo, A.J. (2010). Eosinophilic diseases of the gastrointestinal tract. Scand. J. Gastroenterol. 45, 1013–1021.

Malek, T.R., and Castro, I. (2010). Interleukin-2 receptor signaling: at the interface between tolerance and immunity. Immunity 33, 153–165.

Maloy, K.J., and Powrie, F. (2011). Intestinal homeostasis and its breakdown in inflammatory bowel disease. Nature 474, 298–306.

Manicassamy, S., and Pulendran, B. (2011). Dendritic cell control of tolerogenic responses. Immunol. Rev. 241, 206–227.

Masterson, J.C., Furuta, G.T., and Lee, J.J. (2011). Update on clinical and immunological features of eosinophilic gastrointestinal diseases. Curr. Opin. Gastroenterol. 27, 515–522.

McKarns, S.C., and Schwartz, R.H. (2008). Biphasic regulation of Il2 transcription in CD4+ T cells: roles for TNF-alpha receptor signaling and chromatin structure. J. Immunol. 181, 1272–1281.

Naramura, M., Hu, R.J., and Gu, H. (1998). Mice with a fluorescent marker for interleukin 2 gene activation. Immunity 9, 209–216.

Pulendran, B., Tang, H., and Manicassamy, S. (2010). Programming dendritic cells to induce T(H)2 and tolerogenic responses. Nat. Immunol. 11, 647–655.

Rescigno, M. (2010). Intestinal dendritic cells. Adv. Immunol. 107, 109–138.

Rescigno, M. (2011). Dendritic cells in oral tolerance in the gut. Cell. Microbiol. 13, 1312–1318.

Santaolalla, R., Fukata, M., and Abreu, M.T. (2011). Innate immunity in the small intestine. Curr. Opin. Gastroenterol. 27, 125–131.

Sgouroudis, E., Kornete, M., and Piccirillo, C.A. (2011). IL-2 production by dendritic cells promotes Foxp3(+) regulatory T-cell expansion in autoimmune-resistant NOD congenic mice. Autoimmunity 44, 406–414.

Shembade, N., Ma, A., and Harhaj, E.W. (2010). Inhibition of NF-kappaB signaling by A20 through disruption of ubiquitin enzyme complexes. Science 327, 1135–1139.

Sorrentino, A., Thakur, N., Grimsby, S., Marcusson, A., von Bulow, V., Schuster, N., Zhang, S., Heldin, C.H., and Landström, M. (2008). The type I TGF-beta receptor engages TRAF6 to activate TAK1 in a receptor kinase-independent manner. Nat. Cell Biol. 10, 1199–1207.

Steinman, R.M. (2012). Decisions about dendritic cells: past, present, and future. Annu. Rev. Immunol. 30, 1–22.

Swiatczak, B., and Rescigno, M. (2012). How the interplay between antigen presenting cells and microbiota tunes host immune responses in the gut. Semin. Immunol. 24, 43–49.

Takeda, K., and Akira, S. (2004). TLR signaling pathways. Semin. Immunol. 16, 3–9.

Travis, M.A., Reizis, B., Melton, A.C., Masteller, E., Tang, Q., Proctor, J.M., Wang, Y., Bernstein, X., Huang, X., Reichardt, L.F., et al. (2007). Loss of integrin alpha(v)beta8 on dendritic cells causes autoimmunity and colitis in mice. Nature 449, 361–365.

Walsh, M.C., Kim, N., Kadono, Y., Rho, J., Lee, S.Y., Lorenzo, J., and Choi, Y. (2006). Osteoimmunology: interplay between the immune system and bone metabolism. Annu. Rev. Immunol. 24, 33–63.

Wang, F.L., Qin, W.J., Wen, W.H., Tian, F., Song, B., Zhang, Q., Lee, C., Zhong, W.D., Guo, Y.L., and Wang, H. (2007). TGF-beta insensitive dendritic cells: an efficient vaccine for murine prostate cancer. Cancer Immunol. Immunother. 56, 1785–1793.

Webster, K.E., Walters, S., Kohler, R.E., Mrkvan, T., Boyman, O., Surh, C.D., Grey, S.T., and Sprent, J. (2009). In vivo expansion of T reg cells with IL-2-mAb complexes: induction of resistance to EAE and long-term acceptance of islet allografts without immunosuppression. J. Exp. Med. 206, 751–760.